Deregulated PDGFRα signaling alters coronal suture morphogenesis and leads to craniosynostosis through endochondral ossification

Fenglei He[1] and Philippe Soriano[2]

Department of Cell, Developmental and Regenerative Biology

Icahn School of Medicine at Mount Sinai, New York, NY 10029, USA

[1]Present address:
Department of Cell and Molecular Biology, Tulane University, New Orleans, LA 70118

[2]Corresponding author:
Telephone: (212) 241-4552
Email: philippe.soriano@mssm.edu

Keywords: craniosynostosis, endochondral ossification, receptor tyrosine kinase, neural crest, mesoderm

Summary statement

Over-activation of Pdgfra leads to craniosynostosis of coronal suture via endochondral ossification.

Abstract

Craniosynostosis is a prevalent human birth defect characterized by premature fusion of calvarial bones. In this study, we show that tight regulation of endogenous PDGFRα activity is required for normal calvarium development in the mouse and that deregulated PDGFRα activity causes craniosynostosis. Constitutive activation of PDGFRα leads to expansion of cartilage underlying the coronal sutures, which contribute to suture closure through endochondral ossification, in a process regulated in part by PI3K/Akt signaling. Our results thus identify a novel mechanism underlying calvarial development in craniosynostosis.

Introduction

Bone formation is a complex process in which mesenchymal cells become osteoblasts and lie down bone matrix. There are generally two pathways to form bone. The mesenchymal cells may first form a cartilaginous template which is later replaced by osteoblasts that mineralize into bone, as hypertrophic chondrocytes in the growth plate are thought to be an end state of differentiation. This pathway of endochondral ossification occurs in the axial and appendicular skeleton (Kronenberg, 2003; Ornitz, 2005). Recent studies however have challenged this traditional concept of lineage segregation, as hypertrophic chondrocytes in long bones have been shown by lineage tracing methods to be able to transdifferentiate into osteoblasts (Yang et al., 2014a; Yang et al., 2014b; Zhou et al., 2014). Alternatively, mesenchymal cells can aggregate and directly differentiate into osteoblasts. This pathway of intramembranous ossification is observed in the formation of the flat bones in the skull, collarbones and jaw bones (Hall and Miyake, 2000).

The skull is composed of the neurocranium and the viscerocranium (facial skeleton). The neurocranium plays an important role in encasing and protecting the brain and other sense organs. Both endochondral ossification and intramembranous ossification occur during neurocranium formation. The base of the neurocranium forms through endochondral ossification (McBratney-Owen et al., 2008), while the vault (calvarium) is thought to develop exclusively through intramembranous ossification (Hall and Miyake, 2000). The calvarium is composed of paired frontal bones, paired parietal bones, the squamous region of the occipital bone, and the sutures, the fibrous tissues that separate and joint the calvarial bones. Lineage tracing studies show that the frontal bones are derived from the neural crest, the parietal bones originate from the paraxial mesoderm, while the coronal sutures that separate these bones are heterogeneous but

derive mostly from mesoderm cells (Deckelbaum et al., 2012; Jiang et al., 2002; Lenton et al., 2005; Yoshida et al., 2008). During mouse development, the progenitors of sutures and calvarial bones arise at around embryonic (E) day 11 in the supraorbital regions. These cells undergo active proliferation and differentiation while migrating towards their dorsal destination. They develop coordinately in close proximity to the adjacent dura, a thick membrane that surrounds the brain, and surrounding mesenchymal cells through tissue-tissue interactions (Deckelbaum et al., 2012; Opperman, 2000). In addition, the sutures also serve as a growth site and stem cell niche to support continuous growth of calvarial bones after birth (Zhao et al., 2015).

Deformities of the calvarial bones or sutures usually lead to premature fusion of calvarial bones, or craniosynostosis, a common human birth defect with occurrence of 1/2,500 (Senarath-Yapa et al., 2012; Wilkie and Morriss-Kay, 2001). Craniosynostosis may occur as part of a syndrome or more frequently as isolated (non-syndromic) anomalies (Cohen, 2000). Among the genetic alterations identified in humans, mutations are prevalent in genes encoding receptor tyrosine kinases (RTKs), their ligands or downstream signaling components (Johnson and Wilkie, 2011). These include fibroblast growth factor receptor 2 and 3 (*Fgfr2* and *Fgfr3*), *Ephrin-b1* and *Kras*. Of these, mutations in the *Fgfr2* gene are most frequent and account for 32% of all cases (Johnson and Wilkie, 2011). Such mutations lead to activation of FGFR2 and frequently cause Apert syndrome, which is characterized by bi-coronal synostosis and other defects (Ibrahimi et al., 2005). These studies suggest that RTKs and their common signaling targets may be involved in normal development of calvaria and pathogenesis.

Platelet-derived growth factor receptors (PDGFRs) constitute another family of RTKs. In mouse and human, there are two PDGFRs (α and β) and four PDGF ligands (A-D) (Hoch and Soriano, 2003). While both receptors are required for normal

development and homeostasis (Andrae et al., 2008), PDGFRα is essential in proper neural crest cell development through its downstream PI3K/Akt and Rac1 signaling pathways (Fantauzzo and Soriano, 2014; Fantauzzo and Soriano, 2016; He and Soriano, 2013; Klinghoffer et al., 2002; Soriano, 1997; Tallquist and Soriano, 2003). Of the four ligands, PDGFA and PDGFC are specific endogenous activators of PDGFRα, and inactivating both ligands cause embryonic lethality at midgestation and severe craniofacial malformations, phenocopying *Pdgfra* null mutants (Ding et al., 2004; Soriano, 1997). It has been reported that both PDGFRα expression level and its activity are significantly increased in Apert osteoblasts (Miraoui et al., 2010), and generalized activation of PDGFRα signaling has been shown to lead to craniosynostosis (Moenning et al., 2009).

In the present study, we show that PDGFRα and its ligand PDGFA are expressed in the developing calvarial tissues. Expression of an activatable form of PDGFRα knocked into its own locus leads to abnormal ossification and craniosynostosis of the coronal sutures in neonates. Interestingly, we find that enhanced PDGFRα signaling activity causes abnormal expansion and premature differentiation of cartilage anlagen underlying the coronal sutures, and that endochondral ossification contributes directly to calvarial morphogenesis. Lineage tracing reveals that these chondrocytes derive from both neural crest and mesoderm cells, and activating PDGFRα signaling in chondrocytes, neural crest or mesoderm causes distinct calvarial phenotypes. Further analysis reveals that both PI3K and PLCγ signaling activity are elevated in neural crest cells (NCCs) expressing constitutively active PDGFRα, and that PDGFRα/PI3K signaling is required for normal development of coronal sutures and frontal bones.

Results

Generalized activation of the Pdgfra^{K} allele leads to craniosynostosis and abnormal calvarial bones. To examine the consequence of deregulated PDGFRα activity in calvarial development, we drove expression of a conditionally activatable D842V *Pdgfra* allele utilizing its endogenous promoter by crossing *Pdgfra*$^{+/K}$ knock-in mice (Olson and Soriano, 2009) with the general epiblast deleter line *Meox2Cre* (Tallquist and Soriano, 2000). Because *Pdgfra*$^{+/K}$*; Meox2Cre* mice exhibit perinatal lethality (Olson and Soriano, 2009), we analyzed skeletal preparations at E18.5. In wild-type embryos, the frontal bones and the parietal bones remained separated by coronal sutures (Fig 1A, C). In *Pdgfra*$^{+/K}$*; Meox2Cre* embryos, however, these bones were fused and the coronal sutures were absent (Fig 1B and D; n=5). Alkaline phosphatase (AP) staining of sagittal section through these embryos highlighted differentiating osteoblasts and revealed that in wild-type embryos, the frontal and parietal bones were separated by AP-negative coronal sutures (Fig 1E). In *Pdgfra*$^{+/K}$*; Meox2Cre* embryos, the frontal and parietal bones were fused, as indicated by continuous AP staining across both bones, which also appeared thicker than in the wild-type controls (Fig 1E, F). These results indicate that PDGFRα activity needs to be tightly regulated for normal calvarial osteogenesis and coronal suture development, and that increased PDGFRα activity leads to craniosynostosis of the coronal suture.

PDGFRα and its ligands are expressed in the calvarial rudiments and the coronal sutures. Using *in situ* hybridization and immunohistochemistry, we examined the expression pattern of *Pdgfra* and its endogenous ligands *Pdgfa* and *Pdgfc*. The rudiments of the frontal bones and the parietal bones are composed of differentiating osteoblasts, which we identified using AP and RUNX2 as markers (Fig 2A, D, H and K). *Pdgfa* and *Pdgfc* exhibited differential expression patterns in developing calvarial tissues.

Pdgfa mRNA was expressed in a similar domain to that of AP in the rudiments of the frontal and parietal bones at E13.5 and E15.5 (Fig 2B, E). *Pdgfc* mRNA was expressed in the ectoderm, but was barely detected in the bone rudiments (Fig 2C, F). *Pdgfra* expression, as detected by EGFP expression in *Pdgfra*$^{GFP/+}$ knock-in embryos, was identified in the mesenchymal cells surrounding RUNX2^{+} osteoblasts at E13.5 (Fig 2G, H and I). At E15.5, *Pdgfra* expression overlapped with RUNX2 in some osteoblasts as well as in coronal suture cells (Fig 2J, K and L). Together with the craniosynostosis phenotype observed in *Pdgfra*$^{+/K}$*; Meox2Cre* embryos (Fig 1), these results are consistent with a role for PDGFA-PDGFRα signaling during calvarial development and coronal suture morphogenesis.

Constitutive activation of PDGFRα leads to ossification of coronal sutures and abnormal development of the underlying cartilage. To trace the onset of the *Pdgfra*$^{+/K}$*; Meox2Cre* craniosynostosis phenotype, we analyzed sections across the coronal sutures at different stages. At E13.5, AP activity became detectable in the differentiating osteoblasts within the frontal and parietal bone rudiments, which were separated by the AP-negative coronal sutures through E15.5 (Fig 3A, C and E). In contrast, the coronal sutures of *PDGFRα*$^{+/K}$*; Meox2Cre* embryos showed AP activity by E15.5 (Fig 3B, D and F; n=4 for each stage), suggesting that these sutural cells are transitioning to osteoblasts. In addition, the calvarial rudiments in *Pdgfra*$^{+/K}$*; Meox2Cre* embryos became thicker than in wild type counterparts at E15.5. The AP positive domain exhibited sharp edges flanking AP negative tissues underneath the coronal sutures (Fig 3F). Alcian blue (AB) staining of alternate sections indicated that the AP negative and AB positive cells were cartilage cells, which were observed both in control but significantly more in *PDGFRα*$^{+/K}$*; Meox2Cre* embryos starting at E13.5 (Fig 3G-L). BrdU labeling results showed proliferation rates for mutant chondrocytes (63%) that trended higher than controls

(53.6%; Fig S1, n=9, p<0.01). To confirm the identity of these cartilage cells, we analyzed expression of a series of molecular markers. In situ hybridization results showed that *Sox9* and *Col2a1* were expressed in these cells, indicating that these cells were chondrocytes and that many more chondrocytes were formed in *Pdgfra*$^{+/K}$*; Meox2Cre* embryos (Fig 4A-D). Expression of the hypertrophic chondrocyte marker *Col10a1* was also detected, suggesting these chondrocytes underwent differentiation in both wild type and *Pdgfra*$^{+/K}$*; Meox2Cre* embryos (Fig 4E-F). Expression of osteoblast marker *Ocn* in the *Pdgfra*$^{+/K}$*; Meox2Cre* cartilage indicates that these cells begin to differentiate into osteoblasts (Fig 4G-H). In line with this result, immunohistochemistry showed that the osteoblast markers RUNX2 and OSTERIX were expressed in the chondrocytes of *Pdgfra*$^{+/K}$*; Meox2Cre*, but not in wild type embryos (Fig 4I-L), indicating that activation of PDGFRα signaling promotes endochondral ossification. By E18.5, the chondrocytes underlying the parietal bony rudiments were replaced by AP positive osteoblasts, but some chondrocytes underlying the frontal bone remained (Fig 4M-N). These results indicate that PDGFRα regulates the timing and extent of endochondral ossification during calvarial development, and that constitutive PDGFRα activation promotes chondrocyte formation and subsequent differentiation into osteoblasts.

PDGFRα-directed endochondral ossification contributes to calvarial morphogenesis and coronal suture craniosynostosis. To confirm our observation that endochondral ossification contributes to calvarial morphogenesis in *Pdgfra*$^{+/K}$*; Meox2Cre* embryos, we used *Col2a1Cre* mice which express *Cre* recombinase specifically in chondrocytes (Sakai et al., 2001) to fate map these cells. Lineage tracing with the R26R^{lacZ} reporter line (Soriano, 1999) showed that at E15.5, the *LacZ* reporter was expressed in both the frontal cartilage and the perichondrium underneath the coronal sutures (Fig 5A, C; n=5). At P20, chondrocyte-derivatives were detected in the nasal bones and tissues at the

junctions between calvarial bones, including the coronal sutures (Fig 5E). Compared to littermate controls, *Pdgfra*$^{+/K}$*; Col2a1Cre* embryos exhibited many more chondrocyte-derived cells (Fig 5B, D; n=3), and ectopic chondrocyte-derived tissues adjacent to the coronal sutures at E15.5. At E18.5, skeletal preparations showed enlargement of *Pdgfra*$^{+/K}$*; Col2a1Cre* skulls (Fig S2). The total length of *Pdgfra*$^{+/K}$*; Col2a1Cre* skulls were 6.9%±1.2% ($p<0.01$) larger than wild type, the mutant frontal bones were 11.7%±2.5% ($p<0.01$) longer than the control, and the mutant parietal bones were 3.1%±3% ($p>0.05$) longer than the control (n=5). At P20, *Pdgfra*$^{+/K}$*; Col2a1Cre* mice accumulated more chondrocyte-derived derivatives in the nasal bones and calvarial junctions (Fig 5E, F) and exhibited a domed skull, indicating abnormal calvarial development (Fig 5G, H; n=7). Skeletal preparations revealed abnormal morphology of coronal sutures in *Pdgfra*$^{+/K}$*; Col2a1Cre* mice compared to that in the control littermates (Fig 5I, J). AP staining of sagittal sections of these skulls revealed that *Pdgfra*$^{+/K}$*; Col2a1Cre* frontal and parietal bones were thinner than controls (Fig 5K, L). Further analysis using the R26R^{TdT} reporter (Madisen et al., 2010) for lineage tracing revealed that many cells formerly expressing *Col2a1Cre* in *Pdgfra*$^{+/K}$*; Col2a1Cre* mice were RUNX2 positive and aligned with calvarial osteoblast (Fig 5M, N). These results indicate that ectopic PDGFRα activity in the chondrocyte lineage disrupts normal calvarium development, but does not cause craniosynostosis by P20.

Activating PDGFRα signaling in neural crest or mesoderm leads to distinct phenotypes. The calvarial bones are derived from two different origins, the neural crest and the mesoderm (Chai et al., 2000; Jiang et al., 2000; Yoshida et al., 2008). To examine in which lineage over-active PDGFRα signaling causes craniosynostosis, *Pdgfra*$^{+/K}$ mice were crossed to the *Wnt1Cre-2* (Lewis et al., 2013) or *Mesp1Cre* drivers (Saga et al., 1999). Lineage tracing showed the cartilage underlying the coronal suture was derived

from both neural crest and mesodermal cells (Fig S3). Constitutive activation of PDGFRα in NCCs with *Wnt1Cre-2* led to perinatal lethality. Skeletal preparations of E18.5 *Pdgfra*$^{+/K}$*; Wnt1Cre-2* embryos showed ectopic cartilage formation at the interfrontal, sagittal and coronal sutures (Fig 6A-D; n=7). Lineage tracing revealed that in *Pdgfra*$^{+/K}$*; Wnt1Cre-2; R26R* mice, the neural crest domain expanded posteriorly compared to the control littermates (Fig 6E, F; n=6). Constitutive activation of PDGFRα in mesoderm cells with *Mesp1Cre*, on the other hand, did not cause embryonic lethality. *Pdgfra*$^{+/K}$*; Mesp1Cre* mice survived beyond P20 (n=5) and showed a domed skull (data not shown). Skeletal preparations of *Pdgfra*$^{+/K}$*; Mesp1Cre* mice revealed craniosynostosis of the coronal and lambdoid sutures (Fig 6G, H). At E16.5, ectopic cartilage was observed posterior to the parietal bone (Fig 6I, J), and lineage tracing did not detect a displacement of the mesoderm boundary into the anterior skull, although structures resembling vascular plexus appeared increased in the anterior skull (Fig 6K, L, arrows). These data demonstrate that activating PDGFRα signaling in two distinct lineages leads to different outcomes during calvarial morphogenesis, and that the phenotype observed in *Pdgfra*$^{+/K}$*; Meox2Cre* embryos could be caused by the synergistic effect of over-active PDGFRα activity in both lineages. In addition, the ectopic cartilage at the suture observed using *Wnt1Cre-2* indicates that PDGFRα signaling in NCCs is an important contributor in coronal suture morphogenesis.

PDGFRα engaged PI3K signaling plays a critical role in calvaria development and suture morphogenesis. PDGFRα engages phosphorylation and activation of multiple downstream signaling pathways, including SRC, ERK1/2, STAT, PI3K/AKT and PLCγ pathways. To identify the mechanisms of PDGFRα regulation in NCCs, we assayed the activity of these signaling pathways in primary cultures prepared from E11.5 embryonic frontonasal prominence cells, which are predominantly derived from neural crest.

Western blot analysis revealed that AKT and PLCγ phosphorylation levels were significantly increased in NCCs of *Pdgfra*$^{+/K}$*; Wnt1Cre-2* embryos relative to control littermates (Fig 7A; 1.45±0.14 fold increase in p-Akt and 2.98±0.13 fold increase in p-PLCγ), as observed previously in E13.5 *Pdgfra*$^{+/K}$*; Meox2Cre* whole embryo protein lysates (Olson and Soriano, 2009), while the activity of SRC, ERK1/2 and STAT3 did not change (Fig S4). Immunostaining showed increased phospho-AKT and phospho-PLCγ staining in *Pdgfra*$^{+/K}$*; Meox2Cre* embryos compared to control littermates at E13.5 (Fig 7B-E). PI3K signaling has been established as a critical mediator of PDGFRα signaling during craniofacial and skeletal development (Fantauzzo and Soriano, 2014; Fantauzzo and Soriano, 2016; He and Soriano, 2013; Klinghoffer et al., 2002; Pickett et al., 2008). We therefore asked if activation of PI3K/AKT signaling in NCCs caused abnormal calvarial development. Our results showed that disruption of the PI3K/AKT inhibitor *Pten* in NCCs caused enlargement of the head and calvarial bones (Fig 7F-G) and perinatal lethality (data not shown, n=3). AP and AB staining of *Pten*$^{fl/fl}$*; Wnt1Cre-2* embryos at E14.5 revealed enhanced cartilage formation underlying the coronal sutures, and increased AP signal at the coronal sutures and tissues surrounding the cartilage (Fig 7H, I). Inactivating *Pten* in the whole embryo led to embryonic lethality at E14.5 accompanied by edema, also observed in *Pdgfra*$^{+/K}$*; Meox2Cre* embryos (Olson and Soriano, 2009) (Fig 7J, K). AP staining of the coronal sections showed that the coronal sutures were partially closed and the underlying cartilage was expanded (Fig 7L, M; n=3). In contrast, *Pdgfra*$^{PI3K/PI3K}$ mutant embryos, in which the ability of PDGFRα to activate PI3K signaling is abrogated (Klinghoffer et al., 2002), displayed a wider separation of the frontal and parietal bones at the coronal sutures, and a foramen between the two frontal bones (Fig 7N, O; n=6). AP and AB staining showed hypoplastic cartilage formation in the *Pdgfra*$^{PI3K/PI3K}$ embryos at E15.5 (Fig 7P, Q). Taken together, these results indicate

that PI3K/AKT signaling plays an essential role in calvarial development and coronal suture morphogenesis.

Discussion

Craniosynostosis is a prevalent human birth defect, which arises from genetic or environmental disruptions of normal calvarium development (Wilkie and Morriss-Kay, 2001). Our studies establish PDGFRα and its downstream signaling pathways as crucial regulators of calvarial growth. The calvarial bones are derived from two separate lineages, the neural crest and the mesoderm. Our data showed that increased activity of PDGFRα in both lineages caused abnormal formation of sutures, as well as expansion and premature ossification of the underlying cartilage. We have identified the origin of these cartilage anlagen, and further demonstrate by marker analysis and lineage tracing that upon activation of PDGFRα signaling, cartilage contributes to calvaria morphogenesis through endochondral ossification. We found that this process was under the regulation of PDGFRα-PI3K/Akt signaling in the neural crest lineage. Our study also showed that activating PDGFRα signaling in either the neural crest or the mesoderm caused distinct phenotypes, indicating a synergistic role of signaling in both lineages during calvaria development and craniosynostosis.

A role for PDGFRα in craniosynostosis was first suggested by reports showing increased *PDGFRα* expression and activity in the osteoblasts from patients with Apert syndrome (Miraoui et al., 2010), as well as premature fusion of the interfrontal and coronal sutures by constitutive activation of *PDGFRα* in the neural crest (Moenning et al., 2009). While this particular phenotype is different from the one that we observe at the coronal suture only, it is likely that this is due a difference in the domain or level of expression of the activated PDGFRα, as the earlier study used constitutive expression

from the *ROSA26* locus instead of restricted expression from the endogenous *PDGFRα* locus. Consistent with this interpretation, conditional activation of PDGFRα from these two alleles throughout the epiblast or in NCCs led to different phenotypic outcomes (Kurth et al., 2009; Moenning et al., 2009; Olson and Soriano, 2009). Additional differences in the previous study include the use of a human PDGFRα cDNA which may signal differently than a mouse cDNA, and the use of the original *Wnt1Cre* mice (Danielan et al., 1998) that misexpress *Wnt1*, instead of the *Wnt1Cre-2* driver (Lewis et al., 2013). This may confound some results, as ectopic Wnt signaling activity has been shown to affect normal calvarium development and suture morphogenesis (Liu et al., 2007; Maruyama et al., 2010; Mirando et al., 2010). These differences notwithstanding, both our study and the previous report (Moenning et al., 2009) support an important role for PDGFRα signaling in the regulation of cranial sutures and craniosynostosis. We note however that PDGFRα activation has not been implicated in human patients with craniosynostosis, possibly because PDGFRα activation leads to very pleiotropic phenotypes (Olson and Soriano, 2009).

RTKs regulate cell fates during development and disease by engaging a number of shared intracellular signaling pathways. Among these, the involvement of the ERK1/2 pathway has been well documented in animal models of craniosynostosis. For example, mice carrying active mutations of *Fgfr2* exhibit craniosynostosis correlated with enhanced ERK1/2 signaling activity in the suture cells and osteoprogenitors (Wang et al., 2005; Yin et al., 2008), and inhibiting ERK1/2 phosphorylation or engagement can rescue the craniosynostosis phenotype (Shukla et al., 2007; Eswarakumar et al, 2006). Increased ERK1/2 signaling activity has also been identified in the calvarial bone marrow of *Twist1* mutant mice (Connerney et al., 2008). Interestingly, decreased ERK1/2 signaling activity is also observed in *Epha4*$^{-/-}$ and *Twist1*$^{+/-}$ craniosynostosis models (Ting

et al., 2009). These studies indicate that ERK1/2 signaling must be tightly regulated at multiple stages and in different tissues during calvarium development. Another RTK downstream signaling pathway, PLCγ, is activated with increased PDGFRα activity and has been implicated in osteogenesis of neural crest-derived osteoprogenitors (Moenning et al., 2009; Olson and Soriano, 2009). Our work highlights the role of PI3K/Akt signaling in normal calvarium development and its pathogenesis. In a previous study, we have reported that PDGFAA induces AP activity in mouse embryonic palatal mesenchymal cells via PI3K signaling (Vasudevan et al., 2015). In the present work, we show that PDGFRα engaged PI3K/Akt signaling regulates development of the coronal sutures and underlying cartilage, and deregulated PI3K signaling activity causes ossification of suture cells and expansion of chondrocytes. Together, these data reveal an important role for PI3K/Akt signaling in calvarial development and disease.

Bone can be formed by either endochondral ossification or intramembranous ossification, and it is generally believed that calvaria form only though intramembranous ossification. However, cartilage has also been implicated in calvarial ossification. The parietal cartilage has been shown to be remodeled into membranous bone through a non-endochondral ossification pathway regulated by the membrane-type 1 matrix metalloproteinase (MT1-MMP). In 5 days-old mice, these parietal chondrocytes express chondrocytes marker *Col2a1*, but not the hypertrophic chondrocytes marker *ColX*, and finally undergo apoptosis and are replaced by bone cells by day 10 (Holmbeck et al., 2003). In the present study, we show the existence of cartilage anlagen underlying the coronal sutures derived from both the neural crest and mesoderm (Fig S3). These cells express *Col2a1*, *Sox9* and *Col10a1,* and exhibit AP activity in E18.5 *Pdgfra*$^{+/K}$*; Wnt1Cre-2* embryos, indicating that they contribute to the calvaria via the hypertrophic chondrocyte pathway. Interestingly, this pathway does not necessarily follow the

traditional endochondral ossification process, since we show by lineage tracing using a chondrocyte-specific *Col2a1 Cre* driver that descendants of these cartilage cells are incorporated into calvarial osteoblasts and suture cells at P20 (Fig 5N). This observation is in line with an increasing number of recent studies showing that chondrocytes are not necessarily terminally differentiated, but can instead be transformed into osteoblasts during long bone development (Enishi et al., 2014; Park et al., 2015; Yang et al., 2014a; Yang et al., 2014b; Zhou et al., 2014). We suggest that this alternate differentiation pathway has also been redeployed in calvarial osteogenesis, at least in part under the regulation of PDGFRα. In addition, identification of *Col2a1Cre* lineage-traced cells in the coronal suture suggests that chondrocyte progenitors might be multipotent, since the sutures not only function as connective tissues but also provide growth sites and signaling centers of the growing calvaria (Lana-Elola et al., 2007; Morriss-Kay and Wilkie, 2005; Opperman, 2000). A recent study has identified the suture as a mesenchymal stem cell niche for calvarial bone homeostasis and repair (Zhao et al., 2015). Another recent report also supports this notion by showing that hypertrophic chondrocytes express pluripotency marker genes and are involved in fracture healing (Hu et al., 2017). In addition, since the perichondrium is the major source of osteoblast precursors, expansion of this tissue primordium might contribute to the enhanced growth of calvarial bones in *Pdgfra*$^{+/K}$*; Meox2Cre* mice.

While endochondral ossification occurs in normal posterior frontal suture closure (Moss, 1958; Sahar et al., 2005), deregulated growth factor signaling pathways have been shown to cause ectopic cartilage formation in the anterior frontal, sagittal and lambdoid sutures. For example, ectopic cartilage formation at the sagittal sutures has been reported in mouse models including *Fgfr2*^{S252W} (Holmes and Basilico, 2012; Wang et al., 2005), and *Axin2*$^{-/-}$;*Fgfr1*$^{+/-}$ mutants (Maruyama et al., 2010). Inactivating *Gli3* in

mice causes ectopic cartilage in the lambdoid suture (Rice et al., 2010). Unlike these models, *Pdgfra*$^{+/K}$*; Wnt1Cre-2* embryos exhibit ectopic cartilage in the coronal sutures (Fig 6A-D). The prominent cartilage phenotype in *Pdgfra*$^{+/K}$*; Wnt1Cre-2* could be caused by the persistence and expansion of cartilage that forms transiently within the sutures; alternatively, increased PDGFRα activity might direct mesenchymal stem cell differentiation within the sutures. The fact that we could not phenocopy the ectopic sutural cartilage observed in *Pdgfra*$^{+/K}$*; Wnt1Cre-2* mice using a chondrocyte Cre driver (Fig S2) supports this latter possibility. This notion is further supported by transcriptome analyses showing that PDGF signaling may be involved in directing mesenchymal stem cells differentiation towards a chondrogenic lineage (Ng et al., 2008). These observations, together with other reports that examine the effects of PDGFR activation in fibro/adipogenic progenitors or multipotent perivascular cells, underscore the need for tight regulation of PDGF activity in regulating the homeostatic state of various mesenchymal progenitor cells (Iwayama et al., 2015; Olson and Soriano, 2009; Olson and Soriano, 2011). Together, our findings establish a crucial role for PDGFRα in craniosynostosis, and identify endochondral ossification as a mechanism that can operate during calvarial morphogenesis.

Materials and methods

Mice. All animal experiments were approved by the Institutional Animal Care and Use Committee at Icahn School of Medicine at Mount Sinai. *Pdgfra*^{tm12Sor} (Olson and Soriano, 2009), referred to as *Pdgfra*$^{+/K}$ in the text; *Pdgfra*$^{tm11(EGFP)Sor}$ (Hamilton et al., 2003), referred to as *Pdgfra*$^{+/GFP}$; *Gt(ROSA)26Sor*^{tm1Sor} (Soriano, 1999), referred to as *R26R*^{lacZ}, and *Gt(ROSA)26Sor*$^{tm9(CAG-tdTomato)Hze}$ (Madisen et al., 2010), referred to as R26R^{tdT}, were all maintained on a C57BL/6J background. All other strains, including *Pdgfra*^{tm8Sor} (Tallquist and Soriano, 2003), referred to as *Pdgfra*$^{+/fl}$; *Pdgfra*^{tm5Sor} (Klinghoffer et al., 2002), referred to as *Pdgfra*$^{+/PI3K}$; *Meox2*$^{tm1(cre)Sor}$, (Tallquist and Soriano, 2000) referred to as *Meox2Cre*; *Tg(Wnt1-cre)2Sor* (Lewis et al., 2013), referred to as *Wnt1Cre-2*; *Mesp1*$^{tm2(cre)Ysa}$ (Saga et al., 1999), referred to as *Mesp1Cre*; and *Pten*^{tm1Hwu} (Groszer et al., 2001), referred to as *Pten*$^{+/fl}$, were maintained on C57BL/6J; 129SvJaeSor (MGI:3044540) mixed genetic backgrounds.

Skeletal preparations. Staged embryos were dissected in PBS and sacrificed before their skin and internal organ were removed. Following incubation in 95% ETOH overnight at room temperature, skeletons were stained with 0.015% alcian blue, 0.005% alizarin red, 5% glacial acetic acid, in 70% ETOH for 72 hours at 37°C. The skeletons were then washed briefly in 95% ETOH, cleared with 1% KOH, and subsequently in increasing concentrations of glycerol in KOH until reaching 80% glycerol. For adult mice, the skin was removed using a scalpel, and the cranial base and brain were dissected before staining. Staining and clearing were performed with longer incubation times using the same protocol as for embryos.

X-gal, alcian blue, and alkaline phosphatase staining. For whole-mount staining, the ectoderm and superficial dermis were carefully peeled off, and embryos were fixed and

stained with X-Gal (Soriano, 1999). X-gal staining on cryosections was performed using standard procedures. For alcian blue staining, sections were quickly dipped in 1% alcian blue 8GX (A5268, Sigma) in 0.1N HCl. For alkaline phosphatase (AP) staining, paraffin sections were deparaffinized in Histoclear, rehydrated in decreasing ethanol solutions, and incubated in a solution containing 0.03% nitro-blue tetrazolium chloride (NBT) and 0.02% 5-bromo-4-chloro-3'-indolyphosphate p-toluidine salt (BCIP) to detect AP activity.

In situ hybridization and Immunostaining. In situ hybridization was performed as previously described (He and Soriano, 2013). *Pdgfa* and *Pdgfc* probes were provided by Andras Nagy (Toronto), *Sox9*, *Col2a1* and *Col10a1* probes originate from YiPing Chen (New Orleans), and the *Ocn* probe was from Fanxin Long (St. Louis). Immunostaining was performed according standard protocol using antibodies to anti-phospho-AKT (1:25, Cell Signaling Technology 9271), anti-phospho- PLCγ1 (1:400, Novus Biologicals, MAB74542), RUNX2 (1:1000, Cell Signaling Technology 12556) and OSTERIX (SP7) (1:5000, Abcam, ab94744).

BrdU labeling. BrdU/PBS solution was administered by intraperitoneal (I.P.) injection into pregnant females at 3mg/100g body weight. Embryos were dissected in ice-cold PBS 1 hour after injection. Embryonic heads were fixed in Carnoy's fixative for 1 hour and dehydrated and embedded in paraffin. Immunostaining was performed on 10µm transverse sections using BrdU labeling and detection kit II (Roche, 11299964001) following the manufacturer's instructions. Sections were counterstained with NFR to facilitate quantification. Results from three embryos of each phenotype were collected. Statistical data are presented as mean ± SEM, and subjected to double tailed Student's t-tests.

Western blot. Protein lysates were prepared from primary cultures of frontonasal prominences dissected from E11.5 embryos in RIPA buffer. Western blot was carried out using the primary antibodies from Cell Signaling Technology, Life Technologies and Santa Cruz Biotechnology. Anti-p44/42 MAPK (9102), anti-phospho-p44/42 MAPK (9101), anti-AKT (9272), anti-phospho-AKT (Ser473; 9271), anti-PLCγ (2822), and anti-phospho-PLCγ (2821) were from Cell signaling Technology. Anti-SRC (44-655G) and anti-phospho-SRC (44-660G) were from Life Technologies. Anti-STAT3 (sc-8019) and anti-phospho-STAT3 (sc-8059) were from Santa Cruz Biotechnology. All the primary antibodies were diluted 1:1000 for Western blots. Western blot results were quantified using ImageJ from NIH.

Acknowledgements

The authors thank Tianfang Yang, Tony Chen and Matthew Hung for excellent genotyping work, Francesco Ramirez for the *Col2a1Cre* mice and Greg Holmes for the anti-OSTERIX antibody. We thank our laboratory colleagues and Greg Holmes for constructive comments on the manuscript.

Competing interests

The authors declare no competing or financial interests.

Author Contribution

F.H. designed and performed the experiments and analyzed the data. F.H. and P.S. wrote the manuscript.

Funding

This work was supported by NIH/NIDCR grants R01DE022363 to P.S. and R00DE024617 to F.H.

References

Andrae, J., Gallini, R. and Betsholtz, C. (2008). Role of platelet-derived growth factors in physiology and medicine. *Genes Dev.* **22**, 1276-1312.

Chai, Y., Jiang, X., Ito, Y. and et al. (2000). Fate of the mammalian cranial neural crest during tooth and mandibular morphogenesis. *Development* **127**, 1671-1679.

Cohen, M. M. (2000). *Craniosynostosis. Diagnosis, evaluation and management*. New York: Oxford University Press.

Connerney, J., Andreeva, V., Leshem, Y., Mercado, M. A., Dowell, K., Yang, X., Lindner, V., Friesel, R. E. and Spicer, D. B. (2008). Twist1 homodimers enhance FGF responsiveness of the cranial sutures and promote suture closure. *Dev. Biol.* **318**, 323-334.

Danielian, P. S., Muccino, D., Rowitch, D. H., Michael, S. K. and McMahon, A. P. (1998). Modification of gene activity in mouse embryos in utero by a tamoxifen-inducible form of Cre recombinase. *Curr. Biol.* **8**, 1323-1326.

Deckelbaum, R. A., Holmes, G., Zhao, Z., Tong, C., Basilico, C. and Loomis, C. A. (2012). Regulation of cranial morphogenesis and cell fate at the neural crest-mesoderm boundary by engrailed 1. *Development* **139**, 1346-1358.

Ding, H., Wu, X., Bostrom, H., Kim, I., Wong, N., Tsoi, B., O'Rourke, M., Koh, G. Y., Soriano, P. and Betsholtz, C. (2004). A specific requirement for PDGF-C in palate formation and PDGFR-alpha signaling. *Nat. Genet.* **36**, 1111-1116.

Enishi, T., Yukata, K., Takahashi, M., Sato, R., Sairyo, K. and Yasui, N. (2014). Hypertrophic chondrocytes in the rabbit growth plate can proliferate and differentiate into osteogenic cells when capillary invasion is interposed by a membrane filter. *PLoS ONE* **9**, e104638.

Eswarakumar, V. P., Ozcan, F., Lew, E. D., Bae, J. H., Tome, F., Booth, C. J., Adams, D. J., Lax, I. and Schlessinger, J. (2006). Attenuation of signaling pathways stimulated by pathologically activated FGF-receptor 2 mutants prevents craniosynostosis. *Proc. Natl. Acad. Sci. U. S. A.* **103**, 18603-18608.

Fantauzzo, K. A. and Soriano, P. (2014). PI3K-mediated PDGFRalpha signaling regulates survival and proliferation in skeletal development through p53-dependent intracellular pathways. *Genes Dev.* **28**, 1005-1017.

Fantauzzo, K. A. and Soriano, P. (2016). PDGFRbeta regulates craniofacial development through homodimers and functional heterodimers with PDGFRalpha. *Genes Dev.* **30**, 2443-2458.

Groszer, M., Erickson, R., Scripture-Adams, D. D., Lesche, R., Trumpp, A., Zack, J. A., Kornblum, H. I., Liu, X. and Wu, H. (2001). Negative regulation of neural stem/progenitor cell proliferation by the Pten tumor suppressor gene in vivo. *Science* **294**, 2186-2189.

Hall, B. K. and Miyake, T. (2000). All for one and one for all: condensations and the initiation of skeletal development. *Bioessays* **22**, 138-147.

Hamilton, T. G., Klinghoffer, R. A., Corrin, P. D. and Soriano, P. (2003). Evolutionary Divergence of Platelet-Derived Growth Factor Alpha Receptor Signaling Mechanisms. *Mol. Cell. Biol.* **23**, 4013-4025.

He, F. and Soriano, P. (2013). A critical role for PDGFRalpha signaling in medial nasal process development. *PLoS Genet.* **9**, e1003851.

Hoch, R. and Soriano, P. (2003). Roles of PDGF in animal development. *Development* **130**, 4769-4784.

Holmbeck, K., Bianco, P., Chrysovergis, K., Yamada, S. and Birkedal-Hansen, H. (2003). MT1-MMP-dependent, apoptotic remodeling of unmineralized cartilage: a critical process in skeletal growth. *J. Cell Biol.* **163**, 661-671.

Holmes, G. and Basilico, C. (2012). Mesodermal expression of Fgfr2S252W is necessary and sufficient to induce craniosynostosis in a mouse model of Apert syndrome. *Dev. Biol.* **368**, 283-293.

Hu, D. P., Ferro, F., Yang, F., Taylor, A. J., Chang, W., Miclau, T., Marcucio, R. S. and Bahney, C. S. (2017). Cartilage to bone transformation during fracture healing is coordinated by the invading vasculature and induction of the core pluripotency genes. *Development* **144**, 221-234.

Ibrahimi, O. A., Chiu, E. S., McCarthy, J. G. and Mohammadi, M. (2005). Understanding the molecular basis of Apert syndrome. *Plast. Reconstr. Surg.* **115**, 264-270.

Iwayama, T., Steele, C., Yao, L., Dozmorov, M. G., Karamichos, D., Wren, J. D. and Olson, L. E. (2015). PDGFRalpha signaling drives adipose tissue fibrosis by targeting progenitor cell plasticity. *Genes Dev.* **29**, 1106-1119.

Jiang, X., Iseki, S., Maxson, R. E., Sucov, H. M. and Morriss-Kay, G. M. (2002). Tissue origins and interactions in the mammalian skull vault. *Dev. Biol.* **241**, 106-116.

Jiang, X., Rowitch, D. H., Soriano, P., McMahon, A. P. and Sucov, H. M. (2000). Fate of the mammalian cardiac neural crest. *Development* **127**, 1607-1616.

Johnson, D. and Wilkie, A. O. (2011). Craniosynostosis. *Eur. J. Hum. Genet.* **19**, 369-376.

Klinghoffer, R. A., Hamilton, T. G., Hoch, R. and Soriano, P. (2002). An Allelic Series at the PDGFalphaR Locus Indicates Unequal Contributions of Distinct Signaling Pathways During Development. *Dev. Cell* **2**, 103-113.

Kronenberg, H. M. (2003). Developmental regulation of the growth plate. *Nature* **423**, 332-336.

Kurth, P., Moenning, A., Jager, R., Beine, G. and Schorle, H. (2009). An activating mutation in the PDGF receptor alpha results in embryonic lethality caused by malformation of the vascular system. *Dev. Dyn.* **238**, 1064-1072.

Lana-Elola, E., Rice, R., Grigoriadis, A. E. and Rice, D. P. (2007). Cell fate specification during calvarial bone and suture development. *Dev. Biol.* **311**, 335-346.

Lenton, K. A., Nacamuli, R. P., Wan, D. C., Helms, J. A. and Longaker, M. T. (2005). Cranial suture biology. *Curr. Top. Dev. Biol.* **66**, 287-328.

Lewis, A. E., Vasudevan, H. N., O'Neill, A. K., Soriano, P. and Bush, J. O. (2013). The widely used Wnt1-Cre transgene causes developmental phenotypes by ectopic activation of Wnt signaling. *Dev. Biol.* **379**, 229-234.

Liu, B., Yu, H. M. and Hsu, W. (2007). Craniosynostosis caused by Axin2 deficiency is mediated through distinct functions of beta-catenin in proliferation and differentiation. *Dev. Biol.* **301**, 298-308.

Madisen, L., Zwingman, T. A., Sunkin, S.M., Oh, S.W., Zariwala, H.A., Gu, H., Ng, L.L., Palmiter, R.D., Hawrylycz, M.J., Jones, A.R., Lein, E.S. and Zeng, H. (2010). A robust and high-throughput Cre reporting and characterization system for the whole mouse brain. *Nat Neurosci.* **13** (1):133-40.

Maruyama, T., Mirando, A. J., Deng, C. X. and Hsu, W. (2010). The balance of WNT and FGF signaling influences mesenchymal stem cell fate during skeletal development. *Sci. Signal.* **3**, ra40.

McBratney-Owen, B., Iseki, S., Bamforth, S. D., Olsen, B. R. and Morriss-Kay, G. M. (2008). Development and tissue origins of the mammalian cranial base. *Dev. Biol.* **322**, 121-132.

Mirando, A. J., Maruyama, T., Fu, J., Yu, H. M. and Hsu, W. (2010). beta-catenin/cyclin D1 mediated development of suture mesenchyme in calvarial morphogenesis. *BMC Dev. Biol.* **10**, 116.

Miraoui, H., Ringe, J., Haupl, T., and Marie, P. J. (2010). Increased EFG- and PDGFalpha-receptor signaling by mutant FGF-receptor 2 contributes to osteoblast dysfunction in Apert craniosynostosis. *Hum. Mol. Genet.* **19**, 1678-1689.

Moenning, A., Jager, R., Egert, A., Kress, W., Wardelmann, E. and Schorle, H. (2009). Sustained platelet-derived growth factor receptor alpha signaling in osteoblasts results in craniosynostosis by overactivating the phospholipase C-gamma pathway. *Mol. Cell. Biol.* **29**, 881-891.

Morriss-Kay, G. M. and Wilkie, A. O. (2005). Growth of the normal skull vault and its alteration in craniosynostosis: insights from human genetics and experimental studies. *J. Anat.* **207**, 637-653.

Moss, M. L. (1958). Fusion of the frontal suture in the rat. *Am. J. Anat.* **102**, 141-165.

Ng, F., Boucher, S., Koh, S., Sastry, K. S., Chase, L., Lakshmipathy, U., Choong, C., Yang, Z., Vemuri, M. C., Rao, M. S., et al. (2008). PDGF, TGF-beta, and FGF signaling is important for differentiation and growth of mesenchymal stem cells (MSCs): transcriptional profiling can identify markers and signaling pathways important in differentiation of MSCs into adipogenic, chondrogenic, and osteogenic lineages. *Blood* **112**, 295-307.

Olson, L. E. and Soriano, P. (2009). Increased PDGFRalpha activation disrupts connective tissue development and drives systemic fibrosis. *Dev. Cell* **16**, 303-313.

Olson, L. E. and Soriano, P. (2011). PDGFRbeta signaling regulates mural cell plasticity and inhibits fat development. *Dev. Cell* **20**, 815-826.

Opperman, L. A. (2000). Cranial sutures as intramembranous bone growth sites. *Dev. Dyn.* **219**, 472-485.

Ornitz, D. M. (2005). FGF signaling in the developing endochondral skeleton. *Cytokine Growth Factor Rev.* **16**, 205-213.

Park, J., Gebhardt, M., Golovchenko, S., Perez-Branguli, F., Hattori, T., Hartmann, C., Zhou, X., deCrombrugghe, B., Stock, M., Schneider, H., et al. (2015). Dual pathways to endochondral osteoblasts: a novel chondrocyte-derived osteoprogenitor cell identified in hypertrophic cartilage. *Biol Open* **4**, 608-621.

Pickett, E. A., Olsen, G. S. and Tallquist, M. D. (2008). Disruption of PDGFRalpha-initiated PI3K activation and migration of somite derivatives leads to spina bifida. *Development* **135**, 589-598.

Rice, D. P., Connor, E. C., Veltmaat, J. M., Lana-Elola, E., Veistinen, L., Tanimoto, Y., Bellusci, S. and Rice, R. (2010). Gli3Xt-J/Xt-J mice exhibit lambdoid suture craniosynostosis which results from altered osteoprogenitor proliferation and differentiation. *Hum. Mol. Genet.* **19**, 3457-3467.

Saga, Y., Miyagawa-Tomita, S., Takagi, A., Kitajima, S., Miyazaki, J. and Inoue, T. (1999). MesP1 is expressed in the heart precursor cells and required for the formation of a single heart tube. *Development* **126**, 3437-3447.

Sahar, D. E., Longaker, M. T. and Quarto, N. (2005). Sox9 neural crest determinant gene controls patterning and closure of the posterior frontal cranial suture. *Dev. Biol.* **280**, 344-361.

Sakai, K., Hiripi, L., Glumoff, V., Brandau, O., Eerola, R., Vuorio, E., Bosze, Z., Fassler, R. and Aszodi, A. (2001). Stage-and tissue-specific expression of a Col2a1-Cre fusion gene in transgenic mice. *Matrix Biol.* **19**, 761-767.

Senarath-Yapa, K., Chung, M. T., McArdle, A., Wong, V. W., Quarto, N., Longaker, M. T. and Wan, D. C. (2012). Craniosynostosis: Molecular pathways and future pharmacologic therapy. *Organogenesis* **8**, 103-113.

Shukla, V., Coumoul, X., Wang, R. H., Kim, H. S. and Deng, C. X. (2007). RNA interference and inhibition of MEK-ERK signaling prevent abnormal skeletal phenotypes in a mouse model of craniosynostosis. *Nat. Genet.* **39**, 1145-1150.

Soriano, P. (1997). The PDGF alpha receptor is required for neural crest cell development and for normal patterning of the somites. *Development* **124**, 2691-2700.

Soriano, P. (1999). Generalized lacZ expression with the ROSA26 Cre reporter strain. *Nat. Genet.* **21**, 70-71.

Tallquist, M. D. and Soriano, P. (2000). Epiblast-restricted Cre expression in MORE mice: a tool to distinguish embryonic vs. extra-embryonic gene function. *Genesis* **26**, 113-115.

Tallquist, M. D. and Soriano, P. (2003). Cell autonomous requirement for PDGFR in populations of cranial and cardiac neural crest cells. *Development* **130**, 507-518.

Ting, M. C., Wu, N. L., Roybal, P. G., Sun, J., Liu, L., Yen, Y. and Maxson, R. E., Jr. (2009). EphA4 as an effector of Twist1 in the guidance of osteogenic precursor cells during calvarial bone growth and in craniosynostosis. *Development* **136**, 855-864.

Vasudevan, H. N., Mazot, P., He, F. and Soriano, P. (2015). Receptor tyrosine kinases modulate distinct transcriptional programs by differential usage of intracellular pathways. *Elife* **4**.

Wang, Y., Xiao, R., Yang, F., Karim, B. O., Iacovelli, A. J., Cai, J., Lerner, C. P., Richtsmeier, J. T., Leszl, J. M., Hill, C. A., et al. (2005). Abnormalities in cartilage and bone development in the Apert syndrome FGFR2(+/S252W) mouse. *Development* **132**, 3537-3548.

Wilkie, A. O. and Morriss-Kay, G. M. (2001). Genetics of craniofacial development and malformation. *Nat. Rev. Genet.* **2**, 458-468.

Yang, G., Zhu, L., Hou, N., Lan, Y., Wu, X. M., Zhou, B., Teng, Y. and Yang, X. (2014a). Osteogenic fate of hypertrophic chondrocytes. *Cell Res.* **24**, 1266-1269.

Yang, L., Tsang, K. Y., Tang, H. C., Chan, D. and Cheah, K. S. (2014b). Hypertrophic chondrocytes can become osteoblasts and osteocytes in endochondral bone formation. *Proc. Natl. Acad. Sci. U. S. A.* **111**, 12097-12102.

Yin, L., Du, X., Li, C., Xu, X., Chen, Z., Su, N., Zhao, L., Qi, H., Li, F., Xue, J., et al. (2008). A Pro253Arg mutation in fibroblast growth factor receptor 2 (Fgfr2) causes skeleton malformation mimicking human Apert syndrome by affecting both chondrogenesis and osteogenesis. *Bone* **42**, 631-643.

Yoshida, T., Vivatbutsiri, P., Morriss-Kay, G., Saga, Y. and Iseki, S. (2008). Cell lineage in mammalian craniofacial mesenchyme. *Mech. Dev.* **125**, 797-808.

Zhao, H., Feng, J., Ho, T. V., Grimes, W., Urata, M. and Chai, Y. (2015). The suture provides a niche for mesenchymal stem cells of craniofacial bones. *Nat. Cell Biol.* **17**, 386-396.

Zhou, X., von der Mark, K., Henry, S., Norton, W., Adams, H. and de Crombrugghe, B. (2014). Chondrocytes transdifferentiate into osteoblasts in endochondral bone during development, postnatal growth and fracture healing in mice. *PLoS Genet.* **10**, e1004820.

Figures

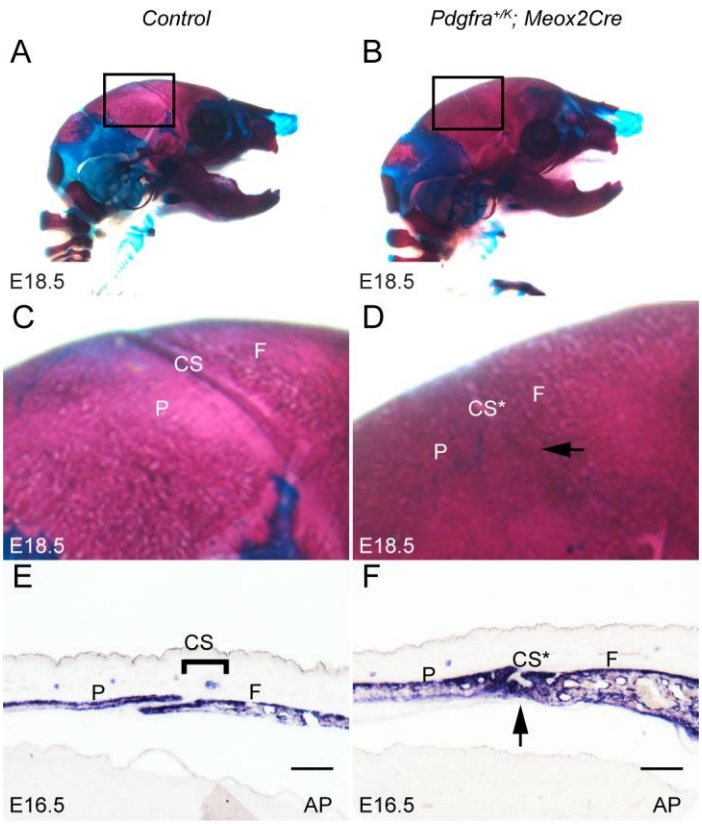

Fig 1. Constitutive PDGFRα activation led to craniosynostosis of coronal sutures. (A, B) Lateral view of skeletal preparations of control littermate (A) and *Pdgfra*$^{+/K}$*; Meox2Cre* (B) embryos (n=5 for each genotype) at E18.5. Bones are stained with alizarin red, and cartilage are stained with alcian blue. (C, D) Magnification of areas defined in A and B showing closed coronal suture in *Pdgfra*$^{+/K}$*; Meox2Cre* embryo (D). (E, F) Alkaline phosphatase (AP) staining of sagittal sections from control littermate (E) and *Pdgfra*$^{+/K}$*; Meox2Cre* (F) embryos (n=5 for each genotype) revealed thickened frontal and parietal bones and closed coronal suture (arrow in F) in the mutant embryo. CS, coronal suture; CS*, fused coronal suture; F, frontal bone; P, parietal bone. Scale bars: 50 μm.

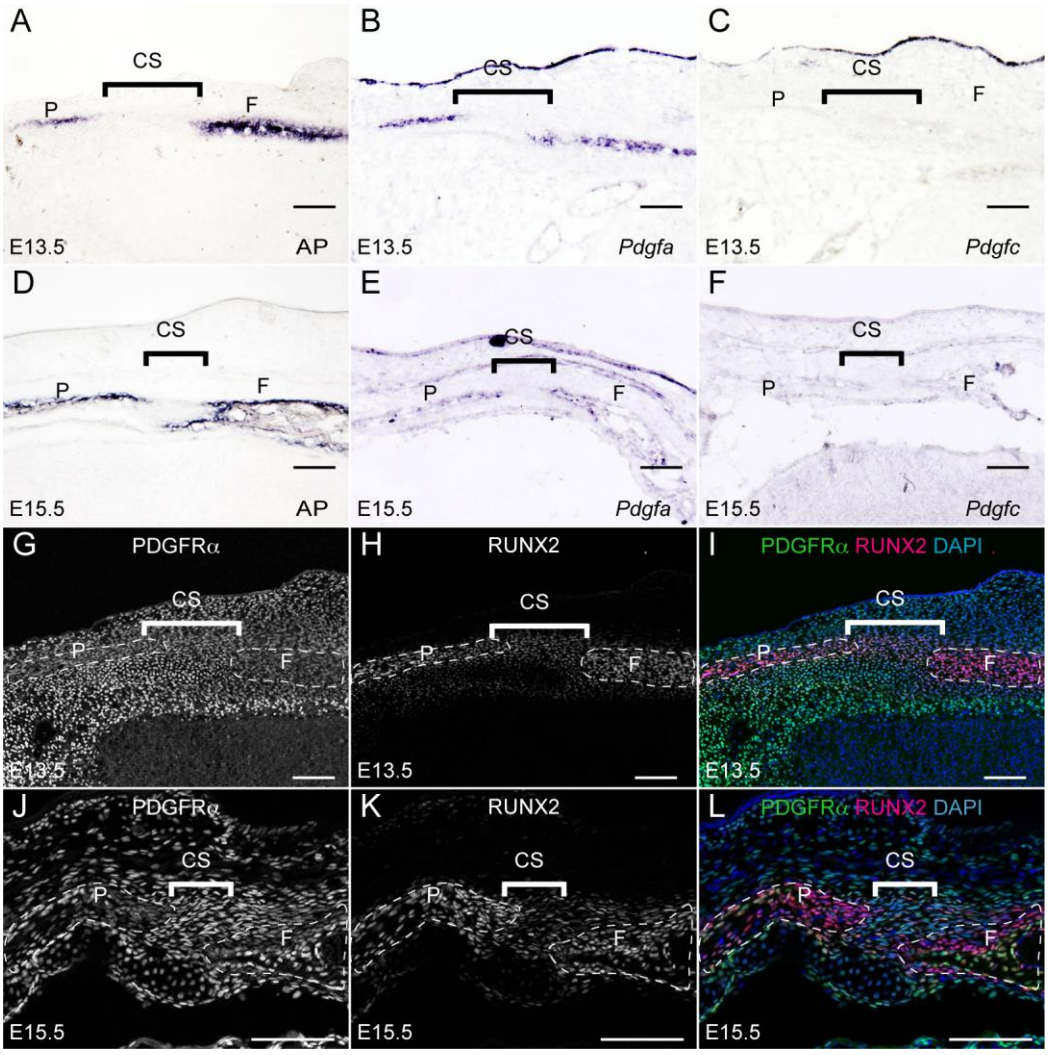

Fig 2. Expression pattern of PDGFRα and its ligands in the developing calvarium. (A, E) AP activity was detected in the osteoprogenitors of the frontal bone and parietal bone on sections through the coronal sutures of E13.5 (A) and E15.5 embryos (D) (n=3 for each stage). (B, E) In situ hybridization showing *Pdgfa* mRNA in the osteoprogenitors of frontal bone and parietal bone in parallel sections of E13.5 (B) and E15.5 (E) (n=3 for each stage) embryonic heads. (C, F) In situ hybridization of *Pdgfc* in parallel sections of E13.5 (C) and E15.5 (F) (n=3 for each stage) embryonic heads. (G, H, I) In coronal sections of E13.5 and E15.5 embryos, expression of *Pdgfra*, as tracked by H2B-GFP in

Pdgfra$^{GFP/+}$ embryos, was detected in the sutural cells and other mesenchymal cells (G, J) surrounding RUNX2^{+} osteoprogenitors (H, K) (n=3 for each stage). Merged images are shown in (I, L). At E15.5, *Pdgfra* expression was identified in the coronal suture, as well as within a portion of endosteal and periosteal osteoprogenitors (yellow cells in L) (n=3). CS, coronal suture; F, frontal bone; P, parietal bone. Scale bars: 50 μm.

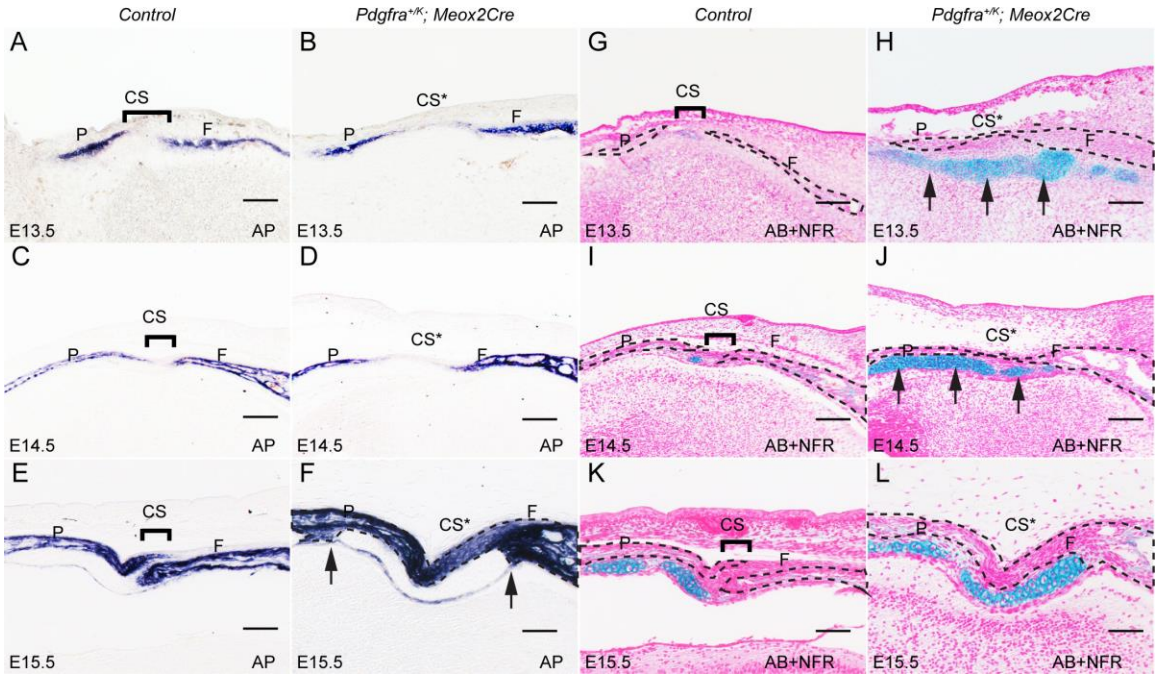

Fig 3. PDGFRα activation leads to premature closure of coronal sutures and ectopic cartilage formation. (A-F) AP staining on coronal sections of control littermate and *Pdgfra*$^{+/K}$*; Meox2Cre* embryo at E13.5 (A, B), E14.5 (C, D), and E15.5 (E, F) at comparable levels (n=4 for each stage). Arrows point to the boundaries of thickening frontal bones and parietal bones in *Pdgfra*$^{+/K}$*; Meox2Cre* embryo at E15.5. (G-L) Alcian blue (AB) staining on parallel coronal sections of control littermate and *Pdgfra*$^{+/K}$*; Meox2Cre* embryos at E13.5 (G, H), E14.5 (I, J) and E15.5 (K, L). Sections were counterstained with nuclear fast red (NFR). Arrows point to ectopic cartilage formed in *Pdgfra*$^{+/K}$*; Meox2Cre* embryos (H, J). CS, coronal suture; CS*, fused coronal suture; F, frontal bone; P, parietal bone. Scale bars: 50 μm.

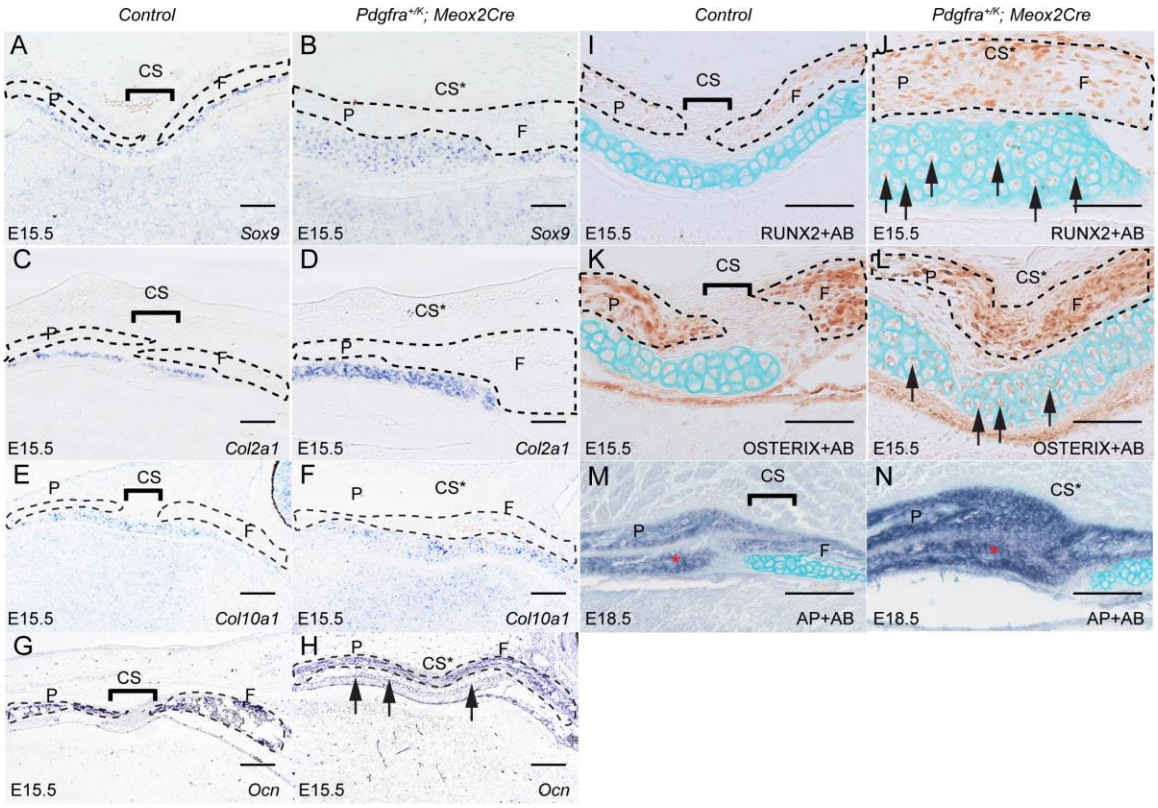

Fig 4. Increased PDGFRα activity promotes endochondral ossification during calvaria development. (A-F) *In situ* hybridization shows expression of chondrocyte markers *Sox9* (A, B) and *Col2a1* (C, D), hypertrophic chondrocyte marker *Col10a1* (E, F), and osteoblast marker *Ocn* (G, H) in coronal sections of littermate control (A, C, E, G) and *Pdgfra*$^{+/K}$*; Meox2Cre* (B, D, F, H) embryos at E15.5 (n=3). Arrows in H point to weak Ocn expression in cartilage. (I-L) Expression of osteogenic markers Runx2 (I, J) and Osterix (K, L) in coronal sections of littermate control (I, K) and *Pdgfra*$^{+/K}$*; Meox2Cre* (J, L) embryos at E15.5 (n=3). Arrows in J and L point to differentiating osteoblasts. (M, N) AP staining in coronal sections of littermate control (M) and *Pdgfra*$^{+/K}$*; Meox2Cre* (N) embryos at E18.5 (n=4). Asterisks represent bones with AP-positive osteoblasts. Sections G-L were stained with AB following immunohistochemistry staining. CS, coronal suture; CS*, fused coronal suture; F, frontal bone; P, parietal bone.

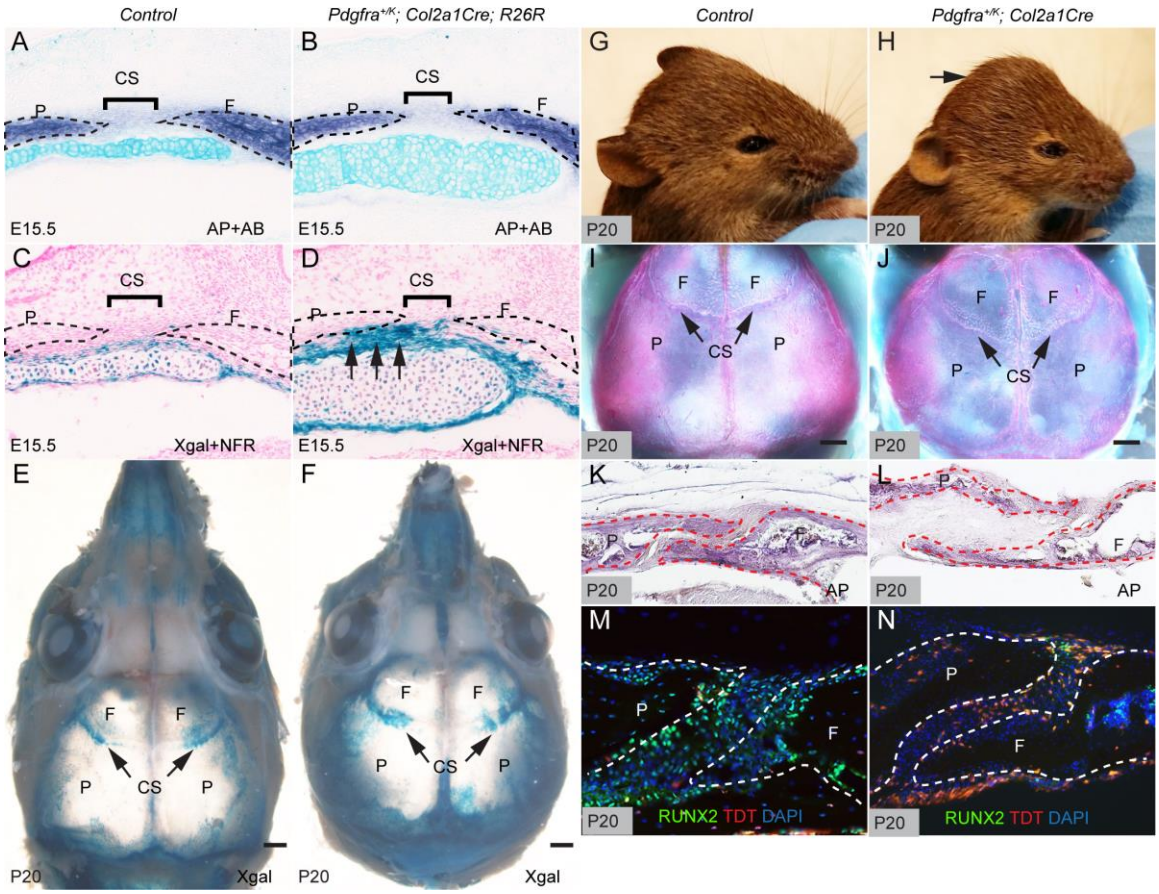

Fig 5. Augmentation of PDGFRα activity in the chondrogenic lineage leads to cartilage expansion and calvarial deformity. (A, B) Double staining of AP and AB on coronal sections of littermate control (A) (n=5) and *Pdgfra*$^{+/K}$*; R26R*$^{+/-}$*; Col2a1Cre* (B) embryos (n=3) at E15.5. (C-F) X-gal staining showing derivatives of chondrogenic lineage on coronal sections of littermate control (C) and *Pdgfra*$^{+/K}$*; R26R*$^{+/-}$*; Col2a1Cre* (D) embryos at E15.5 (counter stained with NFR), and in whole mount heads of P20 littermate control (E) (n=5) and *Pdgfra*$^{+/K}$*; R26R*$^{+/-}$*; Col2a1Cre* (F) mice (n=5). Arrows in D point to chondrocyte-derivatives underlying the coronal suture. (G, H) Lateral views of littermate control (G) (n=7) and *Pdgfra*$^{+/K}$*; Col2a1Cre* (H) mice (n=7) at P20. Arrow points to the domed skull of the mutant mouse (H). (I, J) Dorsal view of skull preparations

following removal of the brain of littermate control (I) (n=5) and *Pdgfra* $^{+/K}$*; Col2a1Cre* (J) (n=5) mice at P20. Bones are stained with alizarin red, and cartilages were stained with alcian blue. Note deformation of the coronal sutures, shown by arrows. (K, L) AP staining on coronal sections of littermate control (K) (n=3) and *Pdgfra*$^{+/K}$*; Col2a1Cre* (L) mice (n=3) at P20. (M, N) Immunofluorescence staining of anti-Runx2 antibody (green) on sagittal sections of *Col2a1Cre; R26R*$^{+/tdT}$ (M) (n=3) and *Pdgfra*$^{+/K}$*; Col2a1Cre; R26R*$^{+/tdT}$ (N) (n=3) skull at P20. CS, coronal suture; F, frontal bone; P, parietal bone. Scale bar= 0.5mm.

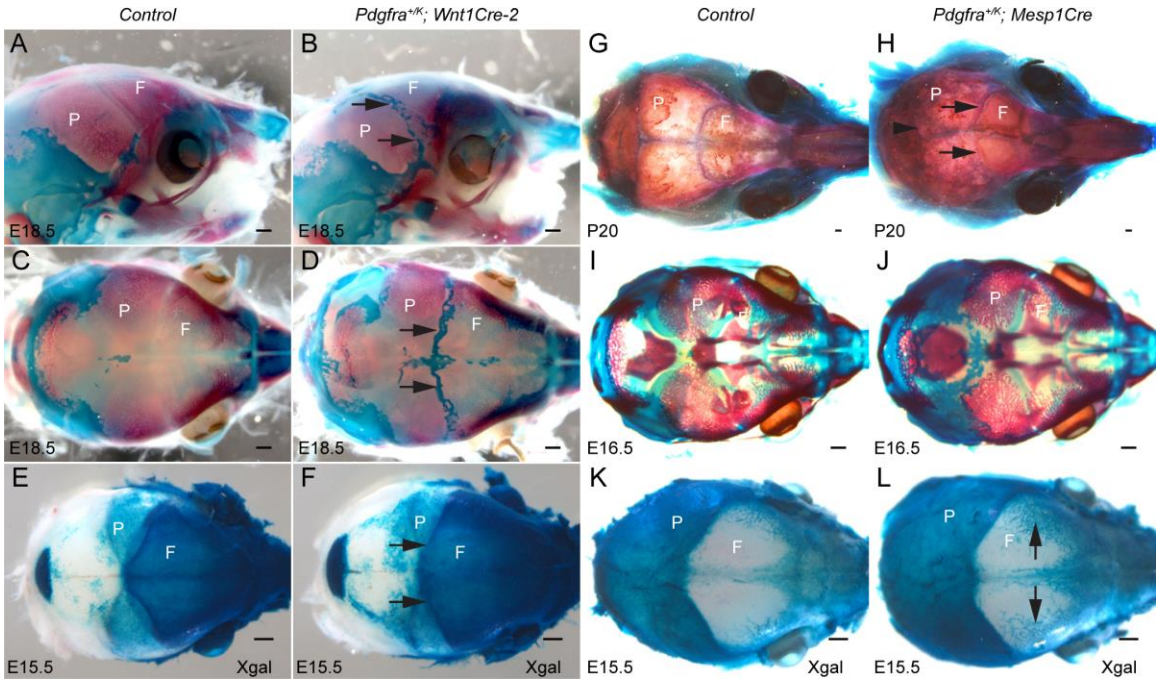

Fig 6. Activation of PDGFRα in the neural crest cells or mesoderm gives rise to distinct calvarial phenotypes. (A-D) Lateral views (A, B) and dorsal views (C, D) of E18.5 littermate control (A, C) (n=7) and *Pdgfra*$^{+/K}$*; Wnt1Cre-2* (B, D) (n=7) calvaria. Arrows in B and D point to ectopic cartilage formed at the sutures. Bones are stained with alizarin red, and cartilages are stained with alcian blue. (E, F) Dorsal views of calvaria of E15.5 littermate control (E) (n=6) and *Pdgfra*$^{+/K}$*; Wnt1Cre-2; R26R* (F) (n=6) following whole mount X-gal staining. Arrows in F point to the neural crest expansion at coronal sutures. (G-J) Dorsal views of littermate control (G, I) (n=5 for each stage) and *Pdgfra*$^{+/K}$*; Mesp1Cre* (H, J) (n=5 for each stage) calvaria at P20 (G, H) and E16.5 (I, J). Arrowhead in H points to fusion at lambdoid suture. Arrows in H point to fusion at coronal sutures. (K, L) Dorsal views of E15.5 calvaria of littermate control (K) (n=5) and *Pdgfra*$^{+/K}$*; Mesp1Cre; R26R* (L) (n=5) embryos following whole mount X-gal staining.

Arrows in L point to mesoderm staining in vascular plexus-like tissues. CS, coronal suture; F, frontal bone; P, parietal bone. Scale bar= 0.5mm.

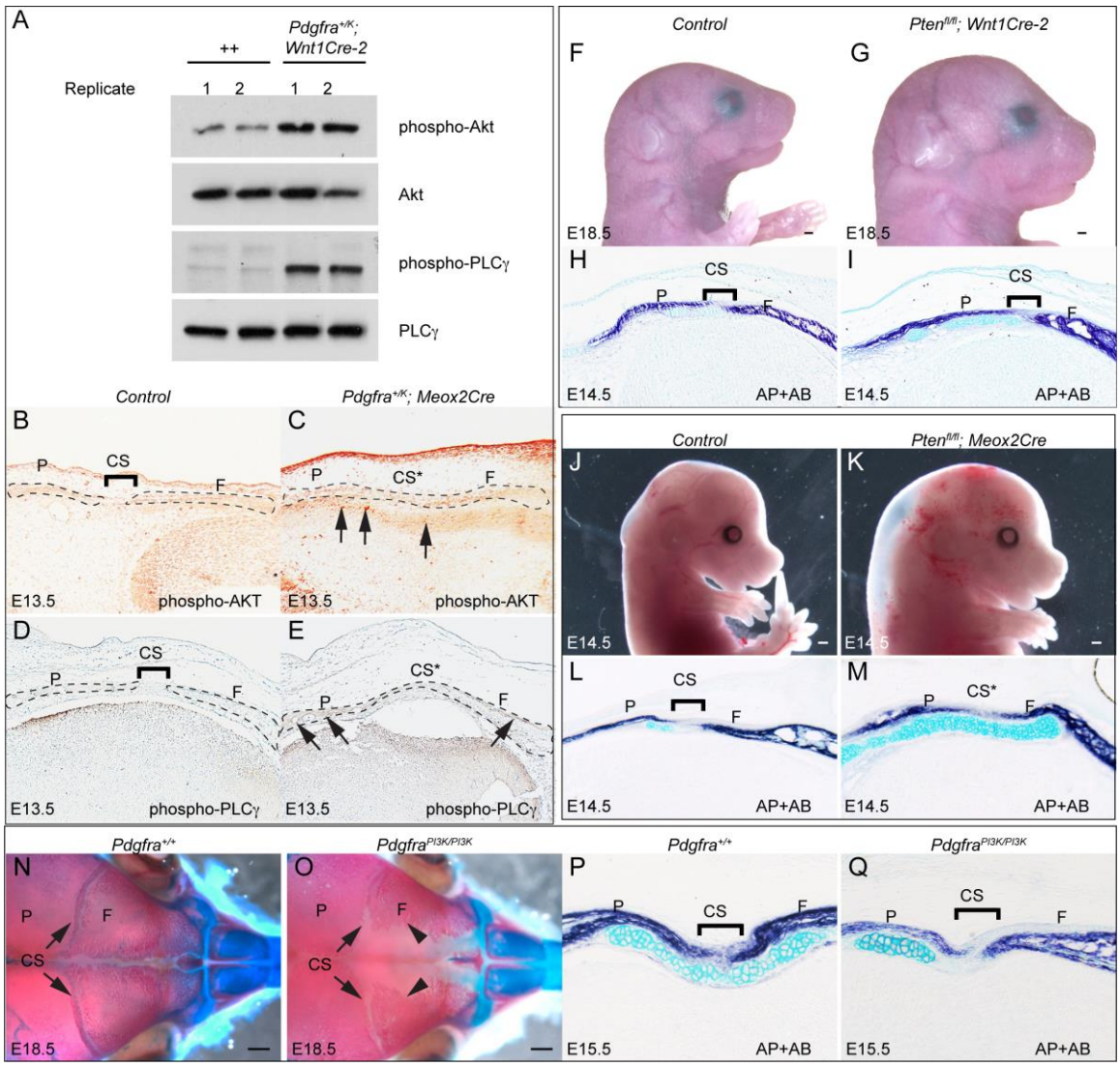

Fig 7. PI3K signaling was implicated in development of frontal cartilage and coronal sutures. (A) Western blot of phospho-AKT, total AKT, phospho-PLCγ, and total PLCγ in primary E11.5 littermate control and *Pdgfra*$^{+/K}$*; Wnt1Cre-2* frontonasal prominence cells. (B-E) Immunostaining of phospho-AKT (B, C) and phospho-PLCγ (D, E) of coronal sections from E13.5 littermate control (B, D) (n=3) and *Pdgfra*$^{+/K}$*; Meox2Cre* (C, E) embryos (n=3). Arrows point to chondrocytes showing increased level of phospho-AKT staining. (F, G) Lateral views of E18.5 littermate control (F) (n=3) and

Pten$^{fl/fl}$*; Wnt1Cre-2* (G) (n=3) embryos. (H, I) Double staining of AP and AB on coronal sections of E14.5 littermate control (H) (n=4) and *Pten*$^{fl/fl}$*; Wnt1Cre-2* (I) (n=4) embryos. (J, K) Lateral views of E14.5 littermate control (J) (n=4) and *Pten*$^{fl/fl}$*; Meox2Cre* (K) (n=4) embryos. (L, M) Double staining of AP and AB on coronal sections of E14.5 littermate control (L) (n=3) and *Pten*$^{fl/fl}$*; Meox2Cre* (M) (n=3) embryos. (N, O) Dorsal views of skeletal preparations of E18.5 littermate control (n=6) and *Pdgfra*$^{PI3K/PI3K}$ (O) (n=6) embryos. Bones are stained with alizarin red, and cartilages are stained with alcian blue. (P, Q) Double staining of AP and AB on coronal sections of E15.5 littermate control (P) (n=3) and *Pdgfra*$^{PI3K/PI3K}$ (Q) (n=3) embryos. CS, coronal suture; CS*, fused coronal suture; F, frontal bone; P, parietal bone. Scale bar=0.5mm.

Supplementary information

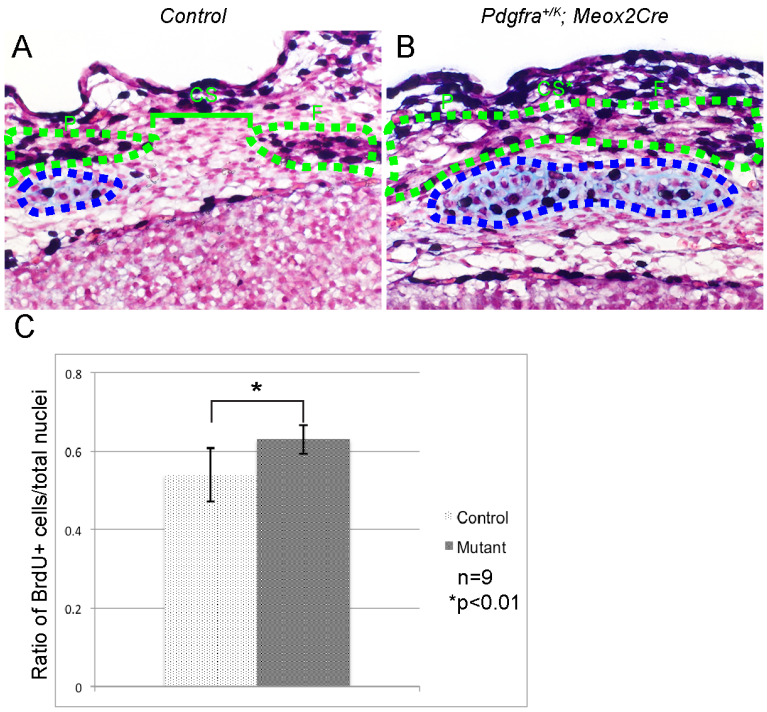

Figure S1. BrdU labeling of coronal suture and the underlying cartilage in E13.5 embryos.

(A, B) BrdU labeling on coronal sections of littermate control (A) (n=9) and *PDGFRα$^{+/K}$; Meox2Cre* (B) embryos (n=9) at E13.5. Sections were counterstained with alcian blue and NFR. (C) Quantification of the proliferation rate of chondrocytes underlying the coronal suture (circled area by blue dashed lines in A and B). Data are presented as mean ± SEM and subjected to double tailed Student's t-tests. CS, coronal suture; F, frontal bone; P, parietal bone.

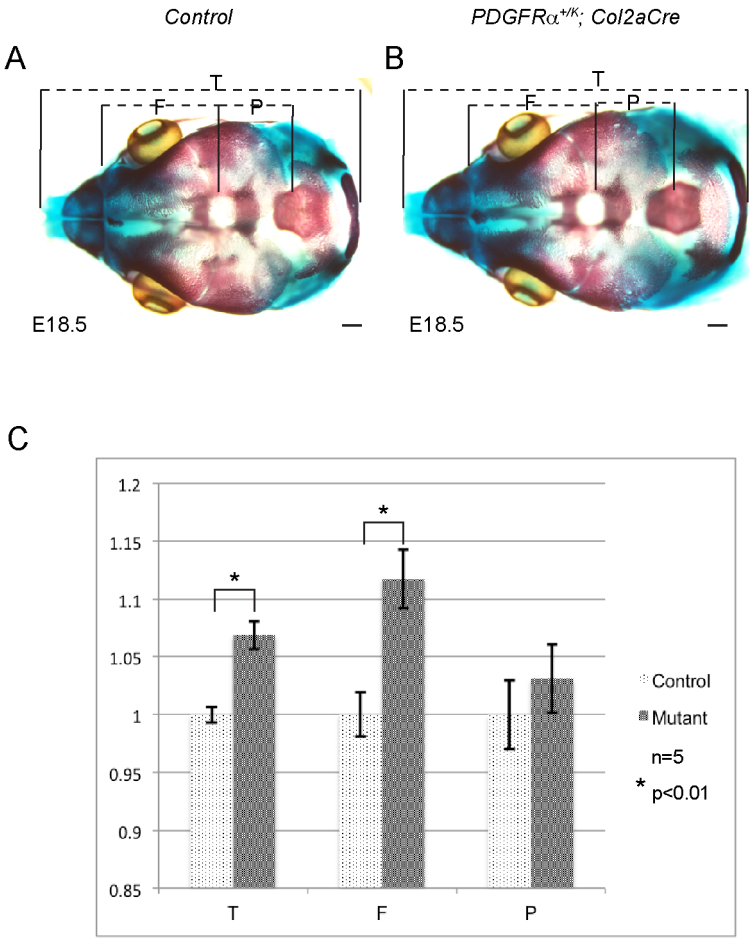

Figure S2. Skeletal preparations of littermate control and *Pdgfra*$^{+/K}$; *Col2aCre* at E18.5.

Dorsal views of skeletal preparations of E18.5 littermate control (A) (n=6) and *Pdgfra*$^{+/K}$*; Col2aCre* (B) (n=5) calvaria. (C) Quantification and statistical analysis of littermate control and *Pdgfra*$^{+/K}$*; Col2aCre* skull morphometry. Data are presented as mean ± SEM and subjected to double tailed Student t-tests. F, frontal bone; P, parietal bone; and T, total length. Bones are stained with alizarin red, and cartilages are stained with alcian blue. Scale bar=0.5mm.

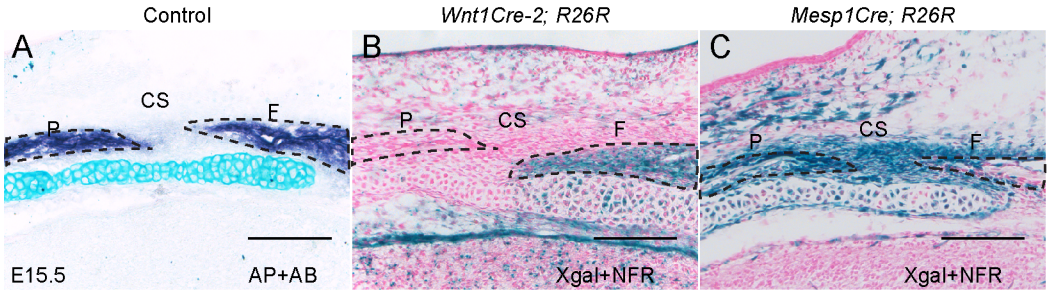

Figure S3. Lineage tracing of the cartilage cells underlying the coronal sutures in E15.5 embryos.

(A) Double staining of AP and AB on coronal section of E15.5 wild type embryo (n=3) across the coronal sutures. (B, C) X-gal staining showing *LacZ* reporter expression (blue) on coronal sections at the same level from E15.5 *Wnt1Cre-2; R26R* (B) (n=3) and *Mesp1Cre; R26R* (C) (n=3) embryos counterstained with NFR. CS, coronal suture; F, frontal bone; P, parietal bone. Scale bars: 50 μm.

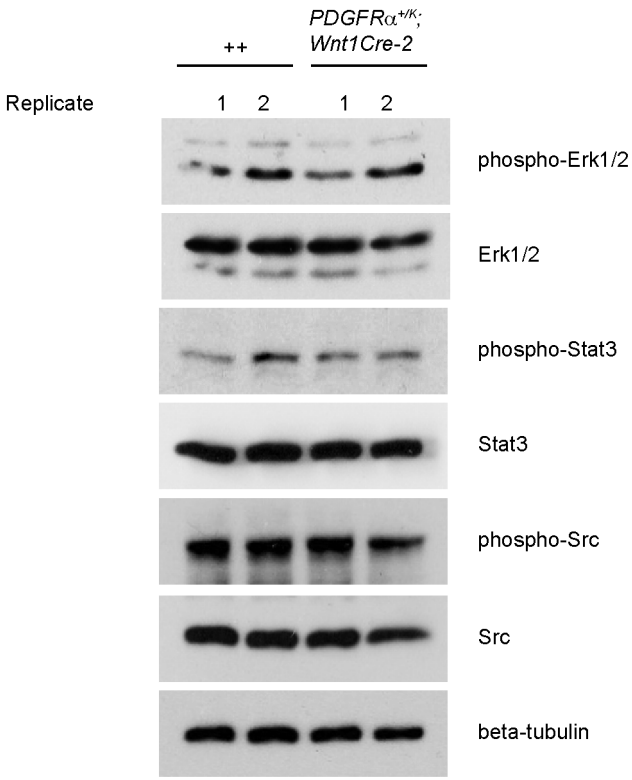

Figure S4. Activity of PDGFRα downstream signaling pathways in FNP lysates.

Western blot of phospho-Erk1/2, Erk1/2, phospho-Stat3, Stat3, phospho-Src, Src and β-tubulin in primary culture of frontonasal prominence cells generated from E11.5 littermate control and *Pdgfra*$^{+/K}$*; Wnt1Cre-2* embryos.